

Microwave treatment and pH influence on hydroxyapatite morphology and structure

A Yudin^{1*}, I Ilinykh¹, K Chuprunov¹, E Kolesnikov¹, D Kuznetsov¹, D Leybo¹ and A Godymchuk^{2,3}

¹Department of Functional Nanosystems and High-Temperature Materials, *National University of Science & Technology "MISIS"*, 4 Leninsky Avenue, Moscow 119049, Russia

²Materials Science Department, *Tomsk Polytechnic University*, 30 Lenina Street, Tomsk 634050, Russia

³Chemistry Environmental Laboratory, *Tobolsk Complex Scientific Station*, Ural Branch of the Russian Academy of Science, 15 Akademician Osipov Street, Tobolsk 626152, Russia

*E-mail: yudin@misis.ru

Abstract. This paper reports the influence of microwave treatment duration and pH conditions of initial precursors on the morphological and crystalline dispersity of the hydroxyapatite (HAp) synthesized by hydrothermal method. The obtained HAp samples were studied by scanning electron microscopy, X-Ray diffraction method and low nitrogen adsorption method. We have obtained nanostructured crystalline hydroxyapatite with 95% crystallinity, porous structure and average particles size in interval 17...46 nm consolidated in aggregates with size distribution of 0.5...25 μm . The pH growth from 8 to 13 results in double increase of HAp specific area (from 69 up to 133 m^2/g), meanwhile microwave irradiation brings to particles aggregation: HAp treated during 0...10...30 min have specific surface are 112...67...41 m^2/g , respectively. As a result at pH=13 and without microwave irradiation treatment we synthesized HAp with maximum surface compared to the surface of natural HAp that makes obtained HAp to be promising material in biotechnological applications.

1. Introduction

Hydroxyapatite is a class of widely used minerals, its chemical composition can be described by the equation $\text{M}_{10}(\text{ZO}_4)_6\text{X}_2$, where M is Ca^{2+} , Mg^{2+} , Sr^{2+} , Ba^{2+} , Mn^{2+} , Fe^{2+} , Zn^{2+} , Cd^{2+} , Pb^{2+} , H^+ , Na^+ , K^+ , Al^{3+} ; ZO_4^- PO_4^{3-} , AsO_4^{3-} , VO_4^{3-} , SO_4^{2-} , CO_3^{2-} , SiO_4^{4-} ; X – OH^- , F^- , Cl^- , Br^- , O^{2-} , CO_3^{2-} , lattice vacancy. Among the others, due to the special properties (crystallinity, crystal dispersity, porosity and stoichiometry) engineered calcium-phosphate apatite or hydroxyapatite ($\text{Ca}_{10}(\text{PO}_4)_6(\text{OH})_2$) [1] has many perspectives as biomedical material to obtain scaffold for tissue engineering [2-4], fillers for healing bone defects [4-6] and drug-delivery systems [7, 8]. Meanwhile, hydroxyapatite (HAp) being a bone component is responsible for spatial grid and porous sponge tissue of bone structure [9-11]. Besides, HAp morphology and crystal size in bone structure depends on bone orientation.

Nanostructured HAp, as previously shown, demonstrates good biocompatible properties to bone tissue, strong osteoblast attachment, high proliferation and particular osteointegration in comparison with micro-sized HAp [3, 8, 12-14]. Nano-scale structure provides perfect sinterability and enhances



densification which and thereby improves mechanical properties of HAp. The morphology, dispersity, specific surface area provides influence on determining drug-delivery properties, loading and releasing properties [15]. Therefore, HAp biocompatibility and mechanical properties may be controlled via stoichiometry, specific surface area, morphology, cristallinity, dispersity, particle size distribution, and agglomeration state [16], and developing method of nanostructured HAp synthesis is of important task in biomedical sector.

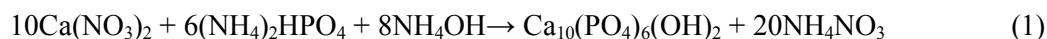
There are many methods of HAp synthesis as sol-gel [17-19], co-precipitation [20-22], hydrothermal [23-25], mechanochemical [26-28], plasma [29], laser ablation [30,31], microwave irradiation [32-34], electrospining [35] and solid-state synthesis [36, 37]. Microwave and hydrothermal methods have attached much interest since they are simple and provide nanostructure and inherent characteristics of the targeted HAp samples. Moreover, the morphology, dispersity, cristallinity and particle size distribution can be controlled via combination of the microwave irradiation and hydrothermal methods.

The aim of this paper is to estimate the influence of pH level and microwave treatment duration on morphology and cristallinity of hydroxyapatite synthesized by hydrothermal method.

2. Materials and Methods

2.1. Hydrothermal synthesis of hydroxyapatite

Calcium nitrate tetrahydrate ($\text{Ca}(\text{NO}_3)_2 \cdot 4\text{H}_2\text{O}$, AR Grade CAS 13477-34-4), diammonium hydrogen phosphate ($(\text{NH}_4)_2\text{HPO}_4$, AR Grade) ammonium hydroxide (NH_4OH , AR Grade, CAS 7664-41-7) produced by Reachem Co (Russia) were used as initial precursors to obtain HAp samples. All HAp samples were synthesized by hydrothermal method under different conditions (table 1). Generally we prepared 10%wt water solutions of all initial precursors by dissolving chemical in distilled water. The diammonium hydrogen phosphate solution was added to the calcium nitrate solution (equation 1).



The obtained suspension was mixed by a mechanical mixer Heidolph RZR 2051 control. The ratio Ca/P was 1.67. The pH level (8, 10, and 13) of mixture was adjusted with 10 weight % NH_4OH solution and monitored by pH-meter MP 230 Mettler Tolloedo. Then 20 ml of suspension was exposed to microwave irradiation in a microwave Anton Paar (Austria) with microwave of 750 W at 150°C during 10, 20 and 30 min (HAp3, HAp4, and HAp5 in table 1).

Table 1. Hydroxyapatites(HAp) synthesized by microwave irradiation assisted hydrothermal method.

Sample	Synthesis conditions	
	pH	Duration of microwave irradiation treatment 750 W, 150 °C, min
HAp#1	8	0
HAp#2	10	0
HAp#3	13	0
HAp#4	10	10
HAp#5	10	20
HAp#6	10	30

2.2. Examination of materials properties

HAp morphology was studied by scanning electron microscope (SEM) Vega 3 (Tescan, Czech Republic). Phase composition and cristallinity were determined by X-Ray diffractometer Difrax 401 (Scientific Instruments, Russia) with the chromium radiation with wave length of 2.2909 Å.

Specific surface area (S) and pore size distribution of samples were studied via low temperature nitrogen adsorption by Brunauer-Emmett-Teller (BET) and Barrett-Joyne-Halenda (BJH) methods, respectively, using Nova 1200 e (Quantachrome, USA). The total pore volume and pore size analysis was made in the relative pressure interval 0.05 – 0.95. Based on specific surface area (S) we calculated average surface size (d) of particles having density of HAp ($\rho=3.16 \text{ g/cm}^3$) by experimental formula (2), used for conditionally spherical particles:

$$d= 6(\rho \cdot S)^{-1}, \quad (2)$$

Particle size distribution was investigated by laser diffraction method with an Analysette 22 (Fritsch, Germany). We sonicated 5 g of each sample in 200 ml of distilled water. Obtained suspension was added at the Analysette 22 droplet by droplet.

3. Results and discussion

According to the patterns of X-Ray analysis all obtained samples include peaks of HAp phase at 2θ of 39, 44, 49, 51, 63, 73, 77 and 84 degrees (HAp#1, HAp#2 and HAp#3, figure 1). The increasing duration of microwave irradiation treatment up to 30 min results in forming of calcium carbonate (peaks at 35, 44 and 50 degrees) in the samples HAp#4, HAp#5 and HAp#6 of the figure 1.

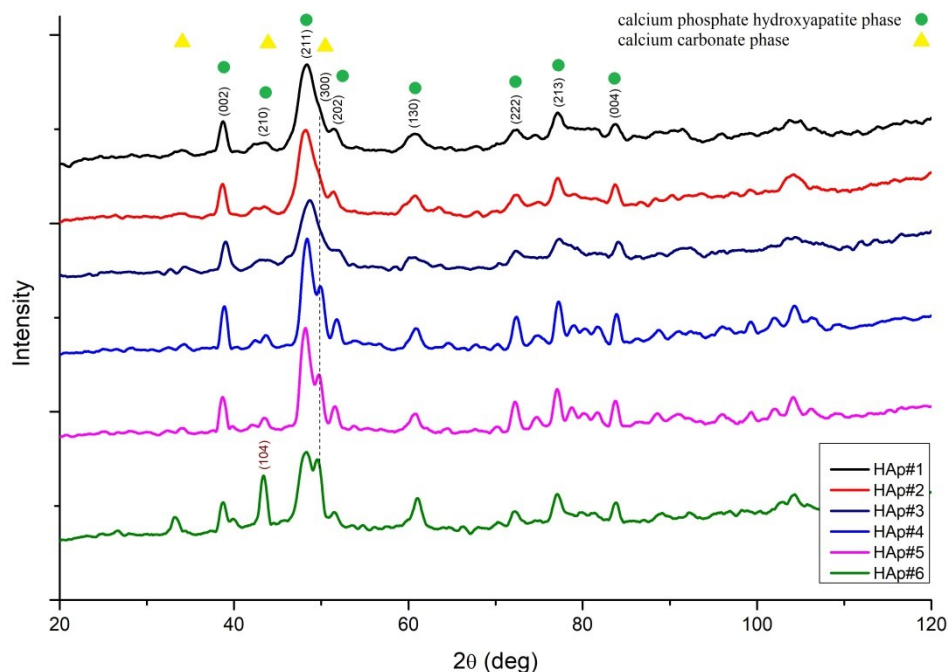


Figure 1. X-Ray patterns of synthesized hydroxyapatites.

Based on SEM analysis we concluded that synthesized HAp's particles have irregular shape (figure 2). The obtained samples mostly consist from aggregates with the average size 0.5-25 μm . The pH change has insignificant influence on HAp' agglomeration: for aggregates it has been observed average size of 4.5 ± 3.6 and $7.5 \pm 6.2 \mu\text{m}$ respectively at pH=8 (HAp#1 on figure 2), pH=10 (HAp#2 on figure 2) and pH=13 (HAp#3 on figure 2).

Microwave treatment obviously leads to deagglomeration since aggregates size decreased from 25 μm (HAp#2, no treatment) to 15 μm (HAp#4, 10 min treatment). Despite slight effect of the treatment on aggregates size, duration did not cause formation of smaller particles (figure 2, HAp#5 and HAp#6). At pH=13 HAp' aggregates consist from the flakes with size from 30 to 500 nm (figure 2, HAp#3).

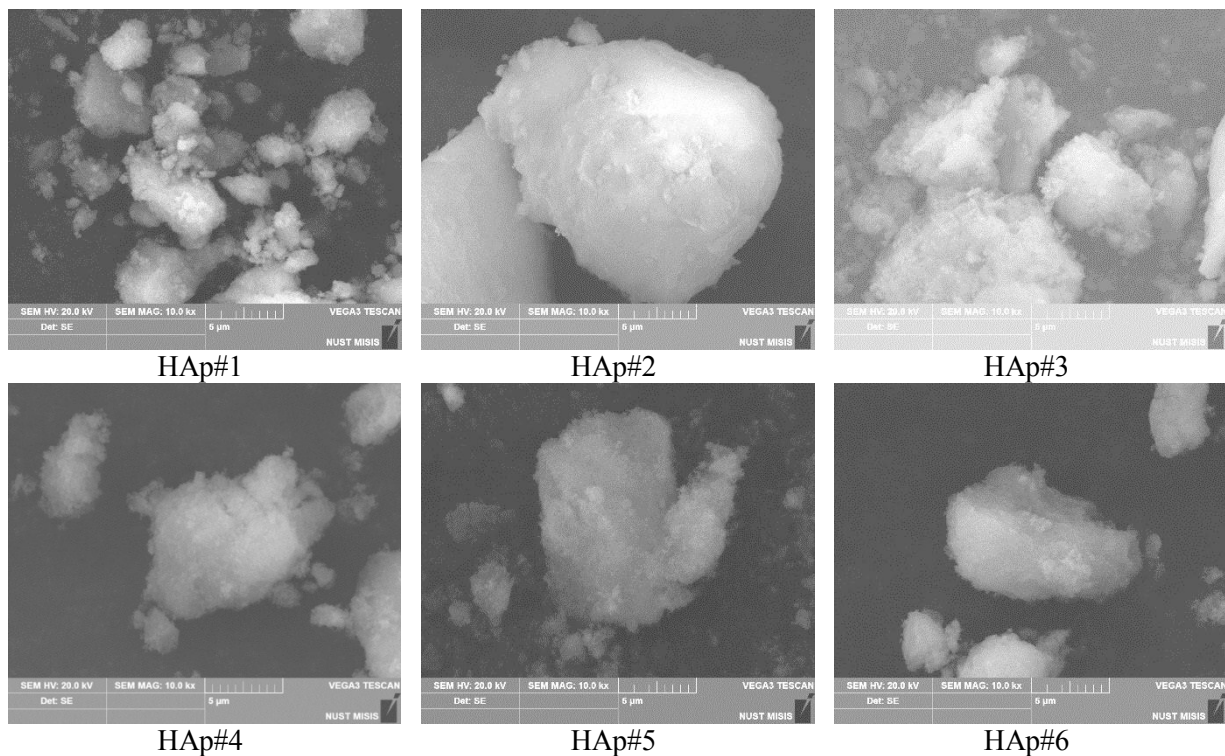


Figure 2. SEM images of hydroxyapatites.

Dispersive analysis has shown that obtained HAp samples have implicit bi-modal distribution with particle size distribution (PSD) in a wide range of 0.5-500 µm (figure 3). It has been revealed that pH value of initial mixture have no effect on the range of particle size distribution (figures 3a, 3b and 3c). Nevertheless at pH=10 there is implicit third peak in the PSD curve at $d=250\mu\text{m}$ (figure 3b, HAp#2) additionally to two peaks at $d=3-5\mu\text{m}$ and $d=50-100\mu\text{m}$ belonging also to PSD measured at pH 8 (figure 3a, HAp#1) and 13 (figure 3c, HAp#3). The formation of large particles at pH=10 is supported by SEM data proving the formation of big aggregates (figure 2, sample HAp#2)

The microwave irradiation treatment results in formatting smaller HAp' structures: we see a slight PSD shift of from 0.5-500 µm (0 min treatment of HAp#2, figure 3b) to 0.5-300 µm (10 min treatment of HAp#4, figure 3d) and 0.5 – 200 µm (20 min treatment of HAp#5). However the treatment duration from 20 to 30 min does not change PSD range, it remains 0.5-200 µm as shown on the figures 3e and 3f.

Based on BET-analysis it has been shown that HAp particles have more developed structures in stronger basic medium (table 2) pH growth from 8 to 13 results in double increase of HAp specific area (table 2, samples HAp#1, HAp#2, HAp#3). Meanwhile, microwave irradiation brings to particles aggregation, proved by decrease of surface value (table 2, sample HAp#4, 10 min of treatment). Moreover, continuation of the treatment may cause further particles consolidation: HAPs treated during 0...10...20...30 min have average size of 17...28...27...46 nm, respectively. As a result at pH=13 and without microwave irradiation treatment (table 2, sample HAp#3) we obtained HAp with maximum surface of 133 m²/g compared to the surface of natural bone mineral in the range of 100-200 m²/g [38].

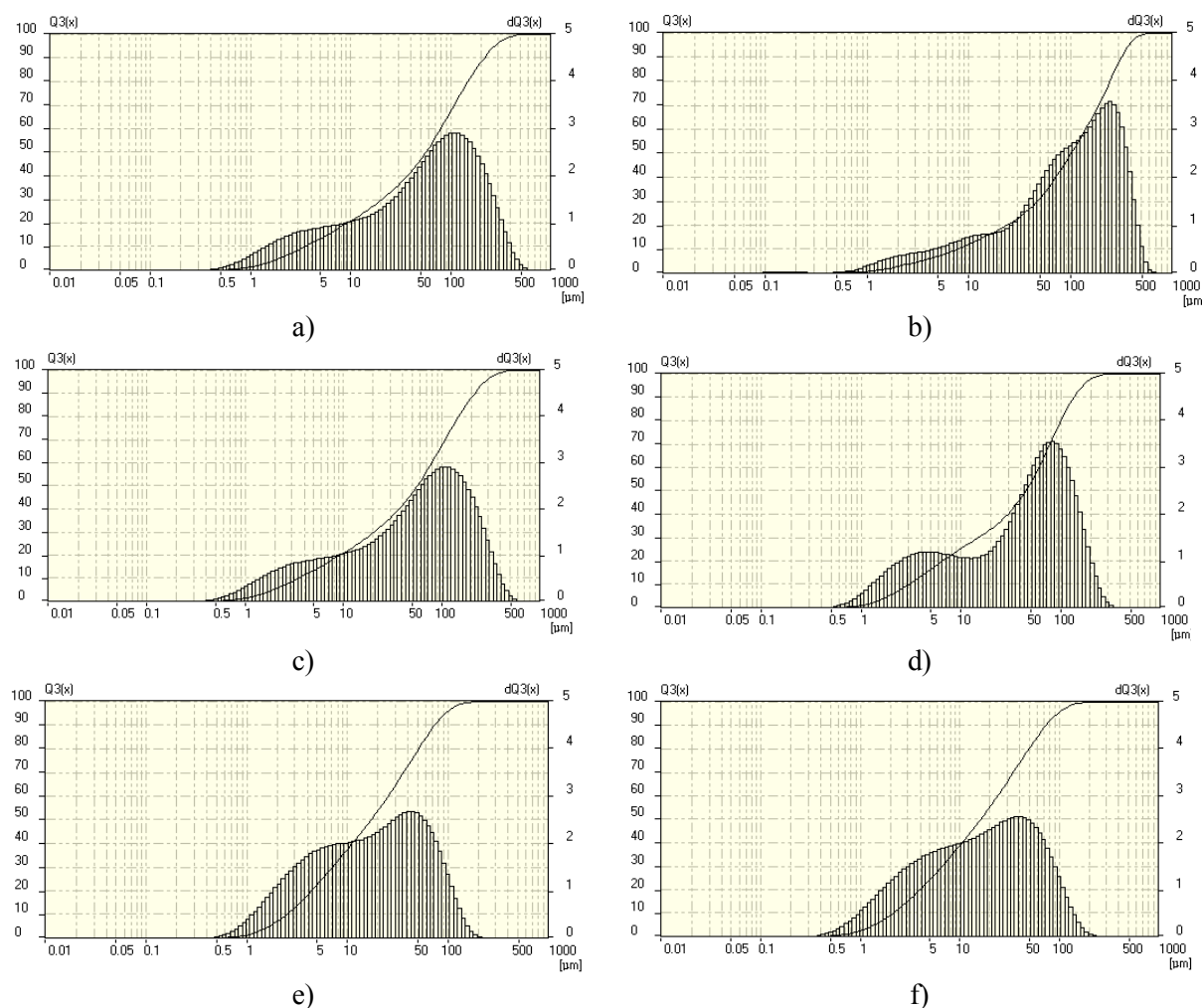


Figure 3. Particle size distribution of synthesized hydroxyapatites at various pH: a) pH=8 (HAp#1), b) pH=10 (HAp#2), c) pH=13 (HAp#3) and different duration of microwave irradiation treatment: b) 0 min (HAp#2), d) 10 min (HAp#4), e) 20 min (HAp#5) f) 30 min (HAp#6).

Table 2. Specific surface area and calculated particles size of obtained hydroxyapatites

Sample name	HAp#1	HAp#2	HAp#3	HAp#4	HAp#5	HAp#6
pH	8	10	13	10	10	10
Duration of treatment, min		0		10	20	30
Specific surface area, m ² /g	69 ± 7	112 ± 11	133 ± 13	67 ± 7	69 ± 7	41 ± 4
Particles size, nm	27	17	14	28	27	46

All investigated samples show the adsorption/desorption isotherms with hysteresis loops attributed to capillary condensation of N₂ in their mesoporous structure (figure 4a). This fact means, that obtained samples have mesoporous structure (figure 4b and 4c). Total pore volume depends on pH and demonstrates maximum for the sample HAp#2 (pH=10) (figure 4b and 4c). Also pH has influence on pore size distribution as it shown on figures 4d and 4e. The pH drop from 13 to 8 provides changes in pore size distribution: peak replaced from 3 to 8 nm for the adsorption data (figure 4d). Further for the desorption data, maximum of the pore size distribution moves from 8 to 5 nm with the increase pH in

interval of 8 – 13 (figure 4e). The microwave irradiation treatment provides agglomeration processes and decreases the total pore volume from 0.3 to 0.2 cm³/g (figures 4d and 4e).

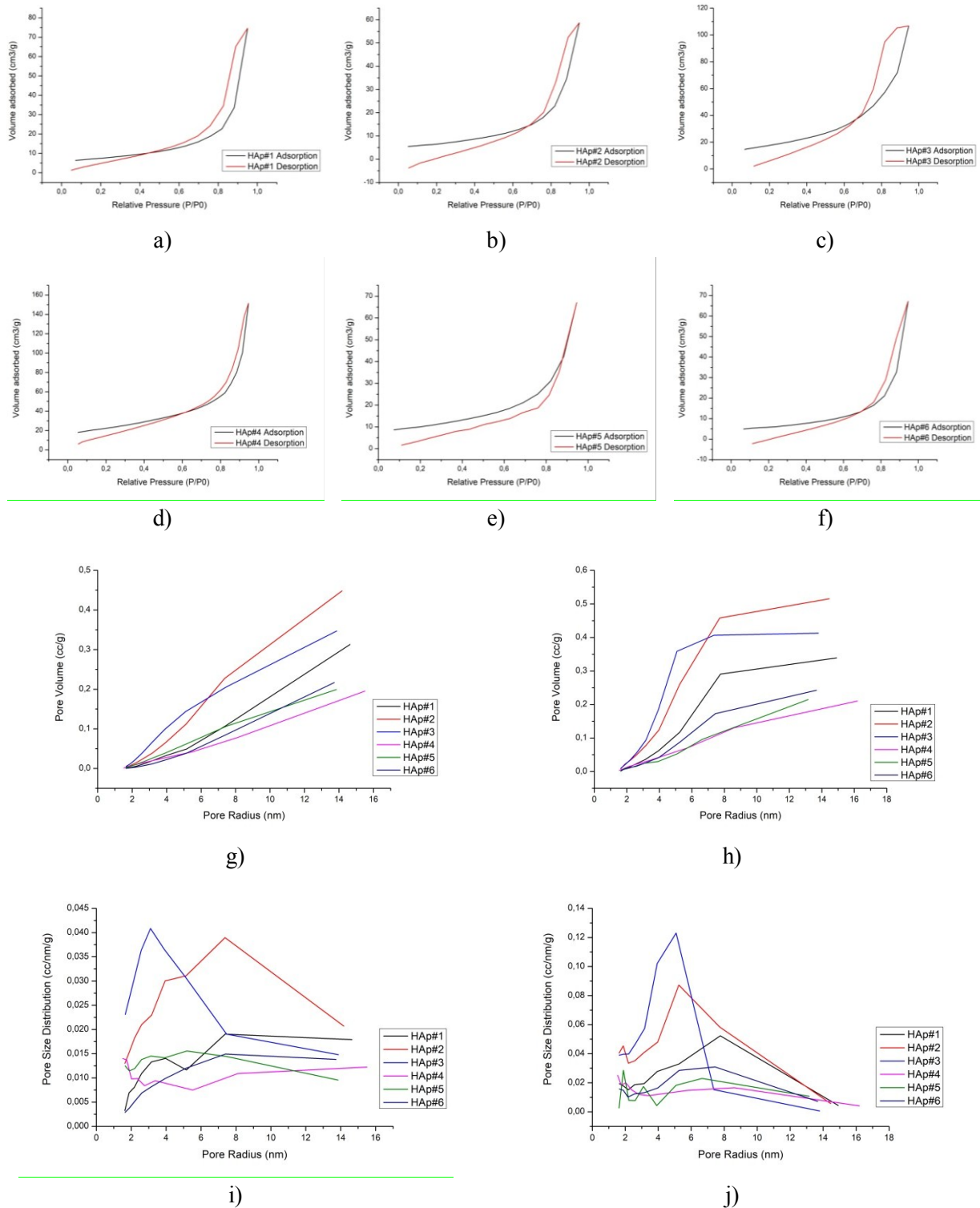


Figure 4. Initial loop hysteresis of HAp#1 (a), HAp#2 (b), HAp#3 (c), HAp#4 (d), HAp#5 (e), HAp#6 (f) total pore volume of HAp samples measured in the processes of adsorption (g), desorption (h) and pore size distribution measured in adsorption (i) and desorption (j).

4. Conclusion

In this paper we have estimated the influence of pH level and microwave treatment duration on morphology and crystallinity of hydroxyapatite synthesized by hydrothermal method. It has been shown that used method helps to obtain nanostructured hydroxyapatite with irregular shape, microporous structure and the maximum total pore volume at maximum level of $0.5 \text{ cm}^3/\text{g}$ and average particles size of 17-46 nm concolidated in aggregates with size distribution of 0.5-25 μm .

Using presented system as a precursor it makes possible to obtain samples with phase composition like one phase HAp and combination of HAp and calcium carbonate phase that is slightly different [38].

However, we have obtained conflicting results concerning pH and treatment duration effect. On the one hand, both conditions bring to the formation of HAp phase. On the other hand, without microwave treatment we have HAp structures with surface of $112 \text{ m}^2/\text{g}$ (at pH=10) compared to $69 \text{ m}^2/\text{g}$ for treated samples. Moreover, continuation of the treatment causes particles consolidation: HAp treated during 0...10...20...30 min have average size of 17...28...27...46 nm, respectively.

The developed synthesis method has allowed producing hydroxyapatite with surface of $133 \text{ m}^2/\text{g}$ close to the surface of natural hydroxyapatite (100-200 m^2/g [38]), that supports to use synthesized material for the tissue engineering scaffolds, drug-delivery systems and bone fillers.

Acknowledgements

The authors acknowledge the financial support of the Ministry of Education and Science of the Russian Federation (Project no. RFMEFI57517X0168).

References

- [1] Okada M and Matsumoto T 2015 Synthesis and modification of apatite nanoparticles for use in dental and medical applications *Jpn. Dent. Sci. Rev.* **51** 85
- [2] MacConnel D 1973 *Apatite, its Crystal Chemistry, Mineralogy, Utilization, and Geologic and Biologic Occurrences* (New York:Spinger-Verlag)
- [3] Vallet-Regi M 2008 *Biomimetic Nanoceramics in Clinical Use: From Materials to Applications* (Cambridge: RSC Publishing)
- [4] Kokubo T 2008 *Bioceramics and their clinical applications* (Woodhead Publishing Limited, Cambridge) 784
- [5] Posner A 1969 The crystal chemistry of bone mineral *Physiol. Rev.* **49** 760
- [6] Okada M 2012 Hydroxylapatite nanoparticles: fabrication methods and medical applications *Sci. Technol. Adv. Mater.* **13** 6
- [7] Dorozhkin S 2010 Nanosized and nanocrystalline calcium orthophosphates *Acta Biomater.* **67** 15
- [8] Hong Y 2010 Fabrication, biological effects and medical applications of calcium phosphate nanoceramics *Mater. Sci. Eng.* **70** 225
- [9] Petit R 1999 The use of hydroxyapatite in orthopaedic surgery: A ten-year review *Eur. J. Orthop. Surg. Traumatol V* **9** 71
- [10] Correia R 1996 Wet synthesis and characterization of modified hydroxyapatite powders *J. Mater. Sci. Mater. Med.* **7** 501
- [11] Sinha A 2008 Polymer assisted hydroxyapatite microspheres suitable for biomedical application *J. Mater. Sci. Mater. Med.* **19** 2009
- [12] Shi Z 2009 Size effect of hydroxyapatite nanoparticles on proliferation and apoptosis of osteoblast-like cells *Acta Biomater.* **5** 338
- [13] Kalita S 2007 Nanocrystalline calcium phosphate ceramics in biomedical engineering *Mater. Sci. Eng. C* **27** 441
- [14] Bose S 2012 Calcium phosphate ceramic systems in growth factor and drug delivery for bone tissue engineering: a review *Acta Biomater.* **8** 1401

- [15] Bose S 2010 Microwave processed nanocrystalline hydroxyapatite: simultaneous enhancement of mechanical and biological properties *Acta Biomater.* **63** 782
- [16] Vijayalakshmi U and Rajeswari S 2012 Influence of process parameters on the sol-gel synthesis of nano hydroxyapatite using various phosphorus precursors *J. Sol-Gel Sci. Technol.* **63** 45
- [17] Omori Y 2014 Fabrication of dispersible calcium phosphate nanocrystals via a modified Pechini method under non-stoichiometric conditions *Mater. Sci. Eng. C.* **42** 562
- [18] Patent US 6426114 B1. Troczynski T 2002 *Sol-gel calcium phosphate ceramic coatings and method of making same* (30, July, 2002)
- [19] Zhang Y 2008 The transformation of single-crystal calcium phosphate ribbon-like fibres to hydroxyapatite spheres assembled from nanorods *Nanotechnol.* **19** 155608
- [20] Okada M 2014 Influence of calcination conditions on dispersibility and phase composition of hydroxyapatite crystals calcined with anti-sintering agents *J. Nanoparticle Res.* **16** 2469
- [21] Lee W-H 2012 Synthesis and characterization of hydroxyapatite with different crystallinity: Effects on protein adsorption and release *J. Biomed. Mater. Res. Part A* **100A** 1539
- [22] Jinawath S 2002 Low-temperature, hydrothermal transformation of aragonite to hydroxyapatite *Mater. Sci. Eng. C* **22** 35
- [23] Zhang G 2011 Preparation of amino-acid-regulated hydroxyapatite particles by hydrothermal method *Mater. Lett.* **65** 572
- [24] Smolen D 2013 Highly biocompatible, nanocrystalline hydroxyapatite synthesized in a solvothermal process driven by high energy density microwave radiation *Int. J. Nanomedicine.* **8** 653
- [25] Fathi M 2009 Fabrication and characterization of fluoridated hydroxyapatite nanopowders via mechanical alloying *J. Alloys Compd.* **475** 408
- [26] Silva C 2007 Crystallite size study of nanocrystalline hydroxyapatite and ceramic system with titanium oxide obtained by dry ball milling *J. Mater. Sci.* **42** 3851
- [27] Briak-Ben Abdeslam H. 2003 Dry mechanochemical synthesis of hydroxyapatites from dicalcium phosphate dihydrate and calcium oxide: A kinetic study *J. Biomed. Mater. Res. Part A.* Company **67A** 927
- [28] Roy M 2010 Bulk Processing of Hydroxyapatite Nanopowder Using Radio Frequency Induction Plasma *J. Am. Ceram. Soc. Blackwell Publishing Inc.* **93** 3720
- [29] Mhin S 2009 Simple synthetic route for hydroxyapatite colloidal nanoparticles via a Nd:YAG laser ablation in liquid medium *Appl. Phys. A.* **96** 435
- [30] Musaev O 2008 Nanoparticle fabrication of hydroxyapatite by laser ablation in water *J. Appl. Phys.* **104** 84316.
- [31] Sadat-Shojai M 2013 Synthesis methods for nanosized hydroxyapatite with diverse structures *Acta Biomater.* **9** 7591
- [32] Yang L 2012 Hydrothermal synthesis of hierarchical hydroxyapatite: preparation, growth mechanism and drug release property *Ceram. Int.* **38** 495
- [33] Ramesh S 2016 Direct conversion of eggshell to hydroxyapatite ceramic by a sintering method *Ceram. Int.* **42** 7824
- [34] Wu Y 2004 Preparation of hydroxyapatite fibers by electrospinning technique *J. Am. Ceram. Soc. Blackwell Publishing Ltd.* **87** 1988
- [35] Fowler B 1974 Infrared studies of apatites. II. Preparation of normal and isotopically substituted calcium, strontium, and barium hydroxyapatites and spectra-structure-composition correlations *Inorg. Chem.* **13** 207
- [36] Ramachandra Rao R 1997 Solid state synthesis and thermal stability of HAP and HAP-TCP composite ceramic powders *J. Mater. Sci. Mater. Med.* **8** 511
- [37] Posner A 1985 The structure of bone apatite surfaces *J. Biomed. Mater. Res.* **19** 241

- [38] Karunakaran G Microwave-assisted hydrothermal synthesis of mesoporous carbonated hydroxyapatite with tunable nanoscale characteristics for biomedical applications *Ceramics International*. In Press <https://doi.org/10.1016/j.ceramint.2018.09.273>